Earth Sci Inform
DOI 10.1007/s12145-016-0258-2

RESEARCH ARTICLE

# Geomorphometric assessment of drainage systems in a semi-arid region of Argentina using geospatial tools and multivariate statistics

**Sibila A. Genchi**[1] · **Alejandro J. Vitale**[2,3] · **Gerardo M. E. Perillo**[2,4] · **María Cintia Piccolo**[1,2]

Received: 23 December 2015 / Accepted: 27 March 2016


**Abstract** In semi-arid environments there is often a lack of data on hydrological variables that limits the ability to understand key hydrological processes. In response to this need, geomorphometric analysis is a quantitative approach that has proven to be useful. This work aims to assess and classify 35 exorheic drainage basins located in a semi-arid area of Argentina (Northeastern Patagonia) according to their geomorphometric properties by using GIS technology and principal component (PCA) and cluster analysis (CA) multivariate techniques. In addition, an assessment of automated drainage network extraction accuracy was performed by comparing it with the actual drainage network. The study showed that it was possible to derive automated drainage networks with errors lower than 6 %. By comparing both PCA and CA, it was found that the former allows a good understanding of the clustering of basins from the CA. All basins were clustered into four groups following a significant spatial continuity. This type of study gives the basis for regional-scale analysis, and provides further information for subsequent modeling.

**Keywords** Geomorphometry · Drainage network extraction · Principal components analysis · Cluster analysis · Semi-arid region · Argentina

Communicated by: H. A. Babaie

**Electronic supplementary material** The online version of this article (doi:10.1007/s12145-016-0258-2) contains supplementary material, which is available to authorized users.

✉ Sibila A. Genchi
genchi.sibila@gmail.com

[1] Departamento de Geografía y Turismo, Universidad Nacional del Sur, B8000FWB Bahía Blanca, Argentina

[2] Instituto Argentino de Oceanografía, CONICET, CC 804, B8000FWB Bahía Blanca, Argentina

[3] Departamento de Ingeniería Eléctrica y de Computadoras, Universidad Nacional del Sur, B8000FWB Bahía Blanca, Argentina

[4] Departamento de Geología, Universidad Nacional del Sur, B8000FWB Bahía Blanca, Argentina

## Introduction

Despite the importance of water in arid and semi-arid environments, there is often a lack of hydrological data (Wheater 2007) that limits the ability to understand key hydrological processes. The use of alternative approaches such as geomorphometric analysis can provide a useful way to overcome the absence of hydrological data. Geomorphometry is the measurement and mathematical analysis of Earth's surface features from digital elevation models (DEM's). Specifically, Strahler (1964) defined morphometric analysis as the measure of the geometric properties of a drainage system. Several previous studies (Youssef et al. 2010; Perucca and Esper 2011; Bali et al. 2011; Sreedevi et al. 2012; Masoud 2014; Vieceli et al. 2014) showed that this approach is capable of describing and predicting basin processes.

A new generation of elevation data generated by remote sensing technologies (e.g., Shuttle Radar Topographic Mission -SRTM-, Interferometric Synthetic Aperture Radar for Elevation -IFSARE-) increased the spatial coverage and resolution. The latter is a promising data source for the computation of topographic (and hydrographic) features in large and remote regions of the world. Geographic information system (GIS) has become an important tool for spatial analysis. The geospatial algorithms in GIS are used to derive terrain parameters from DEM; such algorithms include delineating

Published online: 04 April 2016

watersheds and extracting drainage networks. The most common algorithm is the D8 (i.e., eight flow directions) (O'Callaghan and Mark 1984). By using the D8 algorithm, the drainage network is generated applying a contributing area threshold to the flow accumulation data, which is defined as the minimum drainage area required to initiate a stream. The absence of a method to determine an appropriate threshold as well as the possibility that different thresholds may be better suited to different zones, contribute to increase the uncertainty of network (heads) location (Gatziolis and Fried 2004). However, the use of a constant threshold value is still the most common choice (Jenson and Domingue 1988; Chen and Yu 2011; Thomas et al. 2011), mainly due to the lack of detailed information (Vogt et al. 2003).

As a result of the use of the above technology for studying drainage basins, a large amount of data is available. One way to manage the data generated is by using multivariate statistical analysis, which was successfully applied in numerous hydrographic studies (Wolock et al. 2004; Ali et al. 2010; Ghimire 2014). Within this approach, principal component analysis (PCA) and cluster analysis (CA) are considered to be among the most effective techniques, even over a wide range of environments. Geomorphometric similarities between drainage basins, interpreted in terms of the basin response, constitutes a basis for basins classification. Miller et al. (1990) performed a multivariate analysis of 105 small drainage basins in South-central Indiana, USA; they classified them into five groups by applying CA, and also quantified relations between landforms morphology and lithology by applying PCA. Raux et al. (2011) classified 24 worldwide large drainage basins into three groups according to their hydrogeomorphological parameters and determined those variables that control the hydrosedimentary response using CA and PCA, respectively. Other studies focused on grouping geomorphic parameters (Singh et al. 2009; Subyani et al. 2010; Sharma et al. 2013). As was revealed in Ebisemiju's study (1979), four morphometric statistical studies (Melton 1957; Coates 1958; Mather and Doornkamp 1970; Ebisemiju 1976) carried out in different parts of the world concluded that basin morphology can be largely quantified from the drainage density, stream number, stream length and relief properties.

The Northeastern portion of the Patagonia region (Argentina) is characterized by temperate semi-arid climate and steppe vegetation. It is incised by a complex drainage network (mostly ephemeral) whose origin is associated with late Pleistocene deglaciation. Despite the importance of these drainage systems, which cover a large geographical extent, they have not been studied in detail in the past. The main objective of this paper is to assess and classify 35 exorheic drainage basins located in a semi-arid area (extreme Northeast of Patagonia) (Fig. 1), according to their geomorphometric properties by using GIS technology and PCA and CA multivariate techniques. Prior to this analysis, an assessment of automated drainage network extraction accuracy was performed by comparing it with the actual drainage network. This type of study gives the basis for regional-scale analysis since it can be extended to other drainage systems in Patagonia, as well as provides further information for subsequent modeling.

## Study area

The study area is located in the West coast of San Matías Gulf, in a temperate and semi-arid region. The general tendency of temperature and precipitation exhibits a moderate decrease from coastal to inland areas and from the North to the South. Regarding data for two stations located in the NE (40°45′25″S; 65°01′51″W) and SW (41°26′26″S; 66°14′6″W) portions of the region, the mean annual temperature is 15.6 and 13 °C, respectively; the multi-annual (1980–2009) mean precipitation is 261(NE) and 175 (SW) mm year$^{-1}$. Extreme precipitation events are exceptional; the recorded data (1980–2009) indicated that the peak precipitation amounts reached 102 (NE) and 120 mm (SW) in a 24-h period.

According to the Digital Atlas of the Surface Water Resources of Argentina (SSRH-INA 2002) all the studied basins are part of a hydrographic scheme called "Atlantic-flowing rivers and streams between the Colorado and Chubut rivers". The drainage basins were formed under different paleoclimatic and paleohydrologic conditions (late Pleistocene deglaciation). The streams are ephemeral carrying water during and soon after intense precipitation events. In a very few cases, as occurs in the case of Salado Basin (Fig. 1), partial streams are intermittent or perennial, favored by a spring-fed regime. The water table lies between 60 and 85 m below ground level (Olivares and Sisul 2005).

The overall slope is slightly gentle with some tectonic steps, giving a terraced appearance (Genchi et al. 2011). The landscape geomorphology exhibits a strong association with the geological environment (Genchi 2012). In this sense, the Salado system basically divides the region into two different parts: one located to the North, and the other to the South. The former is mainly characterized by large sedimentary deposits of various sources (e.g., alluvial, colluvial, landslide deposits, etc.) with horizontal to sub-horizontal stratification. Flank pediments and alluvial fans are the dominant geomorphologic features. The latter represents a pre-Cenozoic bedrock subject to compressive, extensional and transcurrent deformations, which comprises (chronologically): crystalline basement rocks poorly exposed, Silurian-Devonian marine deposits, several plutonic associations followed by volcanic-plutonic associations, and ending with essentially volcanic associations

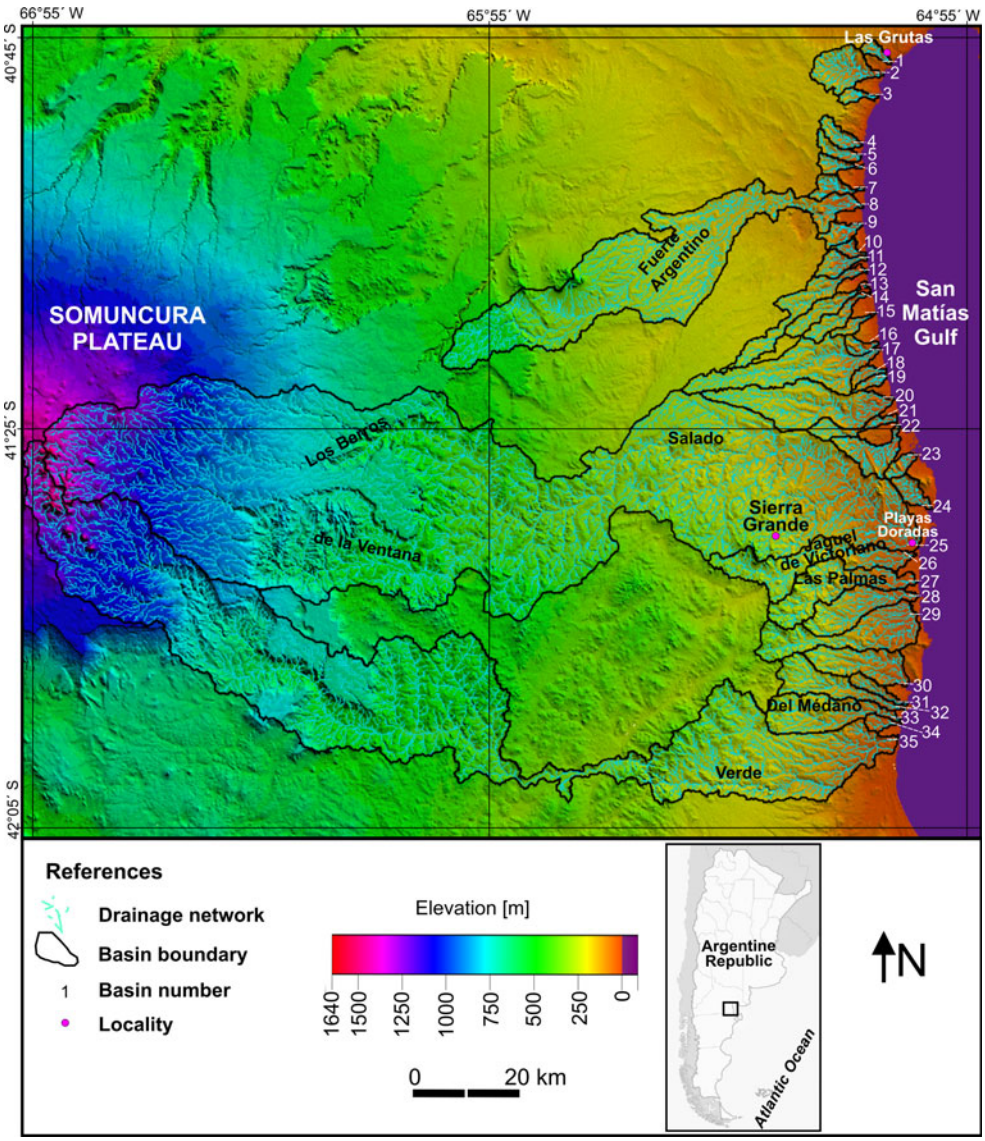


**Fig. 1** Localization of the studied drainage basins

(Appendix). Geomorphologically, this part is dominated by a large exhumed peneplain (González and Malagnino 1984) which is slightly interspersed with unconsolidated sediments. Most of the Western part of the study area comprises a relatively flat basaltic plain (Somuncura Plateau) of Tertiary age (Fig. 1, Appendix).

The soil is classified as Aridisol, typical across the Eastern Patagonia. These skeletal soils have little pedogenetic development and very low organic matter content (<1 %). From a phytogeographical point of view, the study area belongs to the Monte Province (Southern portion) (Cabrera 1976), which is characterized by a shrubby steppe; lower and middle strata (0.5 to 1.5 m) are the most dominant with coverage close to 40 % (León et al. 1998). The study area is minimally impacted by human influences. The main land use consists of extensive sheep ranching. There are few small towns located close to the coastline which are mainly dedicated to tourism.

## Materials and methods

Figure 2 shows the flowchart indicating the main steps of the whole methodology. Below, we describe each of the steps in detail.

### Digital elevation data

In recent years, DEM data derived from remote sensing is being widely used for hydrogeomorphic purposes. The DEM used in the following analysis come from the SRTM, with 90 m spatial resolution. The data was reprojected to Gauss-Krüger projection (zone 3) with WGS84 datum. The DEM dataset is arranged in a regular grid structure (69.04 × 69.04 m). Considering that the DEM, which is generated from remotely sensed data, includes anthropogenic features and the top of the vegetal canopy (Metz et al. 2011), this

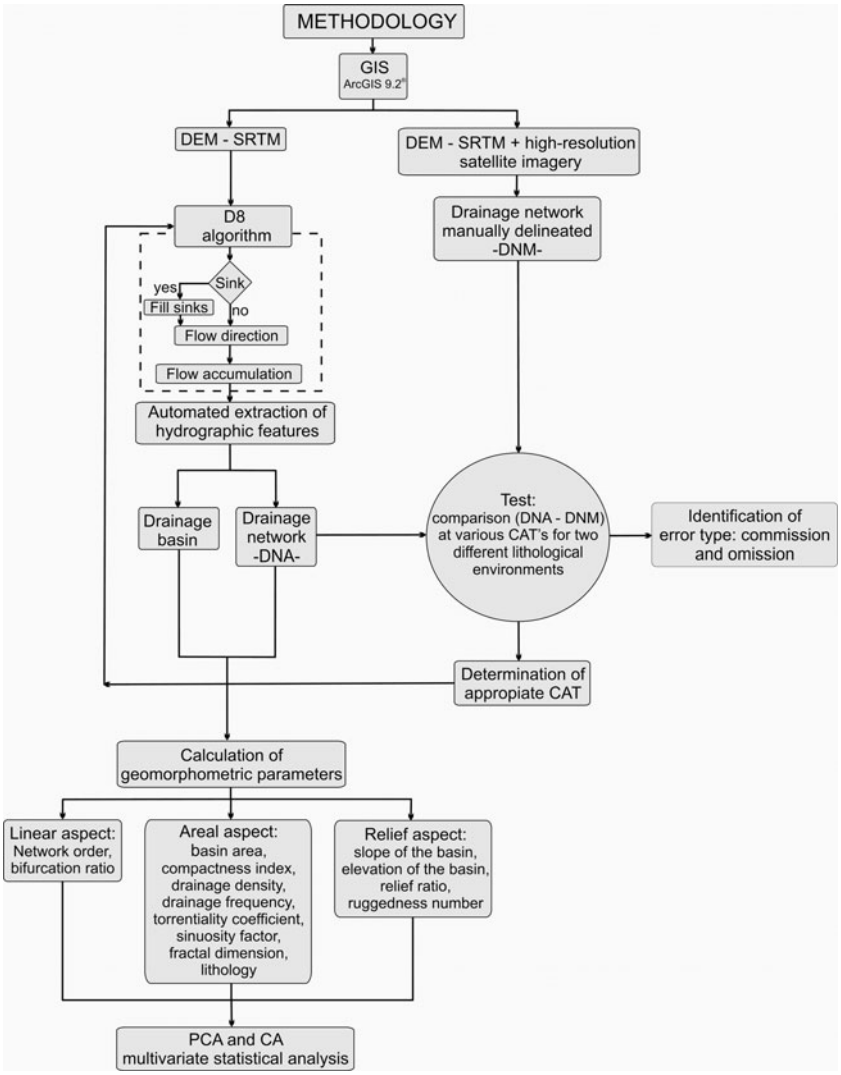


**Fig. 2** Flowchart showing the main steps involved of the whole methodology

does not mean a serious restriction because the study area is slightly anthropized and the vegetal cover is scattered with heights ranging from 0.5 to 1.5 m.

## Automated extraction of hydrographic features from DEM

Extraction of hydrographic features from DEM is based on the gravity concept. In this sense, water flows from higher to lower elevation and it is assumed that there is no interception, evapotranspiration and loss to groundwater (Youssef et al. 2010). The algorithms and models available in GIS-based applications follow a similar processing scheme that evolves: filling of depressions, determination of flow direction and accumulation, drainage network derivation and watershed delineation (Jenson 1991) (Fig. 2).

The *Arc Hydro Tools* in the ArcGIS 9.2® software were used to obtain hydrographic data sets. It employs the D8 single-flow algorithm (O'Callaghan and Mark 1984) in which the downstream side of each grid cell is indicated by one out of the eight directions toward neighboring grid cells (Yamazaki et al. 2009).

### *Drainage network processing*

A correct and precise determination of the drainage network, which is considered de most important hydrologic element, leads to more adequate treatment (Al Rawashdeh 2012). When considering algorithms for drainage networks extraction, the contributing area threshold (CAT) plays a key role. In a regional study, the use of a constant CAT that is independent of landscape conditions implies that the resulting drainage networks may not reflect the actual variability in drainage density (Vogt et al. 2003). In this work, the CAT was determined according to the lithology, since it represents the most variable property, in contrast to vegetation, climate or land use. In addition, it should be noted that drainage pattern, texture and density are influenced in a fundamental way by the

**Table 1** Geomorphometric variables used in the study

| Variable | Formula/symbol |
|---|---|
| [a]Basin area ($km^2$) | $A$ |
| Compactness index (non-dimensional) | $C = 0.28 \frac{P}{\sqrt{A}}$ |
| (Gravelius 1914) | $P$: Basin perimeter (km) |
| Mean slope of the basin (°) | S |
| Standard deviation slope of the basin (°) | $S_{sd}$ |
| [a]Mean elevation of the basin (m) | $H$ |
| [a]Standard deviation elevation of the basin (m) | $H_{sd}$ |
| Relief ratio (non-dimensional) | $R = \frac{\Delta H}{L_b}$ |
| (Schumm 1956) | $\Delta H$: Difference between the highest and the lowest point of the basin (m); $L_b$: Basin length (Max. distance) (km) |
| [a]Ruggedness number (non-dimensional) | $R_n = \Delta HD$ |
| (Schumm 1956) | $D$: Drainage density (km $km^{-2}$) |
| Network order. Hierarchical rank (non-dimensional) | $U$ |
| (Strahler 1957) | |
| Drainage density (km $km^{-2}$) | $D = \frac{L_s}{A}$ |
| | $L_s$: Total stream length (km) |
| Drainage frequency (non-dimensional) | $F = \frac{N}{A}$ |
| | $N$: Stream number |
| Bifurcation ratio (Mean) (non-dimensional) | $B = \frac{N_u}{N_{u+1}}$ |
| (Horton 1945) | $N_u$: Stream number at a given U |
| Torrentiality coefficient (non-dimensional) | $T = \frac{N_{u=1}}{A}$ |
| (Gómez-Villar et al. 2006) | |
| Sinuosity factor (non-dimensional) | $Sin = \frac{L_{ms}}{L_b}$ |
| | $L_{ms}$: Main stream length (km) |

[a] Variables log-transformed (K-S: A = 0.168; H = 0.127; $H_{sd}$ = 0.189; $R_n$ = 0.224)

lithology (Charon 1974; Sener et al. 2005). Therefore, in this work, an appropriate threshold was determined for two clearly different lithological environments, that is, North and South from the Salado System. A set of critical CAT's was considered in order to identify one with the least error for each environment. For this, a comparison of the drainage network automatically extracted (DNA) from SRTM-DEM data by using *Arc Hydro* tool, with the drainage network manually delineated (DNM) from high-resolution satellite imagery (Google Earth, DigitalGlobe © 2013 archive) and also

**Table 2** Value score of each geological unit according to its rock-type erodibility (*Fm* Formation, *C* Complex, *V* Volcanic, *P* Plutonic). See also Appendix

| Rock-type erodibility | Geological units | Score |
|---|---|---|
| Igneous, metamorphic rocks | Mina Gonzalito C; El Jaguelito Fm; Punta Sierra PC; Paileman PC; Marifil VC; Chubut Group; Roca Fm; Colitoro Fm; Somuncurá Fm; Quiñelaf Fm; Curriqueo Fm | 0 |
| Hard-consolidated sedimentary rocks | Sierra Grande Fm; Arroyo Salado Fm; Arroyo Barbudo Fm; El Fuerte Fm; Arroyo Verde Fm; Gran Bajo del Gualicho Fm; Baliza San Matías Fm | 0.25 |
| Weak-consolidated sedimentary rocks | Gaiman Fm; Puerto Madryn Fm; Río Negro Fm; Gran Bajo del Gualicho Fm (half-covered); Rodados Patagónicos Fm | 0.75 |
| Unconsolidated deposits of recent age | Deposits on pediment; piedemont, landslide, colluvial, alluvial, littoral and eolian deposits | 1 |

SRTM-DEM data, was made (Fig. 2). The latter was considered as the reference drainage network.

From comparative analysis between two binary matrix (i.e., absent stream = 0; present stream = 1) belonging to the DNA and DNM, two types of errors were identified: (1) omission error that occurs when the algorithm failed to estimate streams in a grid cell that actually contained them, and (2) commission error when the algorithm detected streams in a grid cell when there were none in that cell.

The error matrix at a given CAT ($E_t$) was produced as follows:

$$E_{ij} = \frac{\left(\sum w_{DNM} - \sum w_{DNA}\right)^2}{(k \times l)^2} \quad (1)$$

$$E_t = \frac{\sum E_{ij}}{m \times n} \quad (2)$$

where $E_{ij}$ corresponds to the error value assigned to the central cell of the moving window (w) of dimension k × l (9 × 9 (i.e., 0.38 km$^2$) and 15 × 15 (i.e., 1.07 km$^2$) cells); m × n is the dimension of the matrix, in terms of the number of rows m, and the number of columns n. Finally, the omission (OE) and commission (CE) errors are discriminated in the following way:

$$if\,(DNM < DNA) \rightarrow CE \quad (3)$$

$$if\,(DNM > DNA) \rightarrow OE \quad (4)$$

## Statistical treatment of geomorphometric data

The study consists of 35 drainage systems with a size greater than 10 km$^2$, located in the West coast of San Matías Gulf (Fig. 1). A set of geomorphometric variables (linear, areal and relief aspects) were measured in each basin (Fig. 2). A detailed description of the variables considered in this work is summarized in Table 1. Moreover, two important variables but relatively little used in hydrography, such as lithology and fractal dimension, deserve special attention in this section.

Rock lithology of the study area offers a different sensitivity to erosion. A score was assigned for each rock type based on level of erodibility as follows: Igneous, metamorphic rocks (score = 0); hard-consolidated sedimentary rocks (score = 0.25); weak-consolidated sedimentary rocks (score = 0.75); and

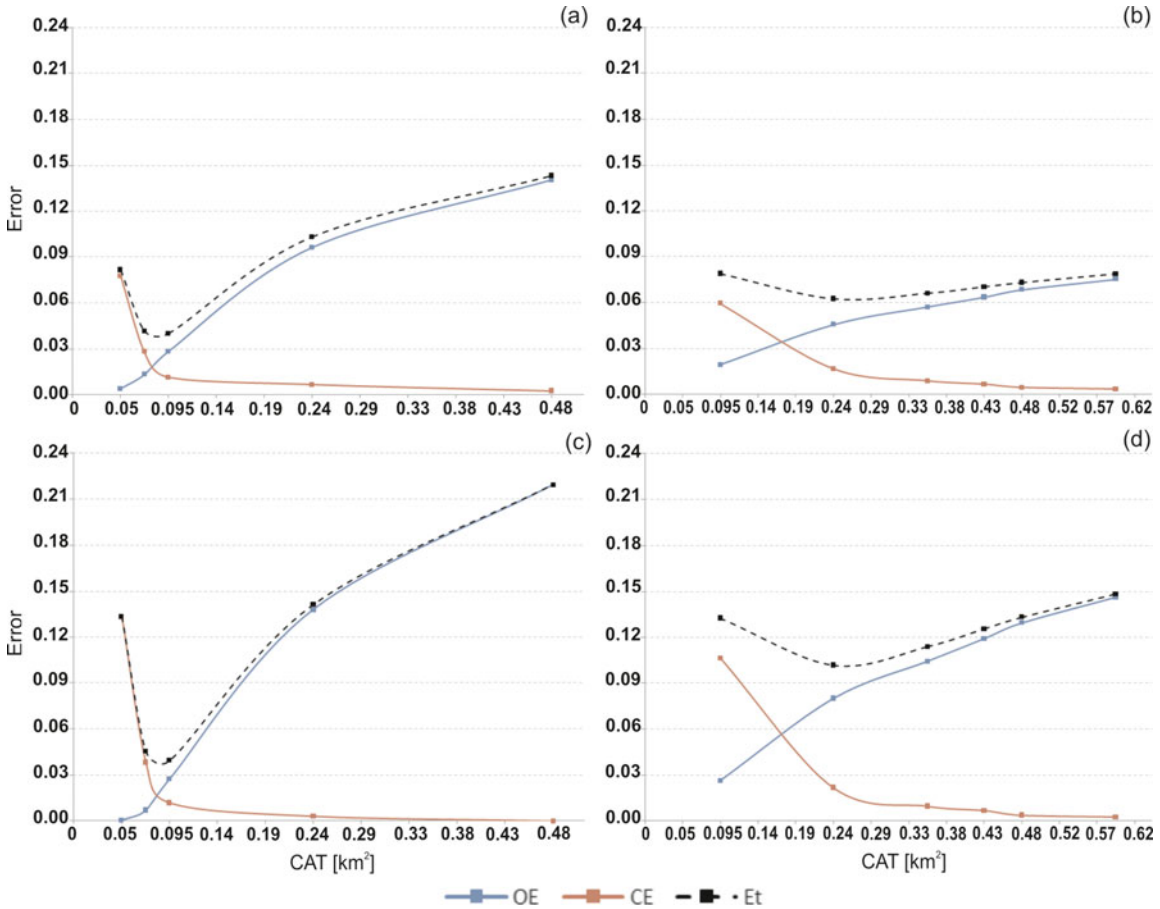


**Fig. 3** Errors (Et, OE and CE) of the DNA at different CAT's for the drainage network located in the North (**a** and **c**) and South (**b** and **d**) of the study area, considering two windows: k × l = 9 × 9 (**a** and **b**) k × l = 15 × 15 (**c** and **d**)

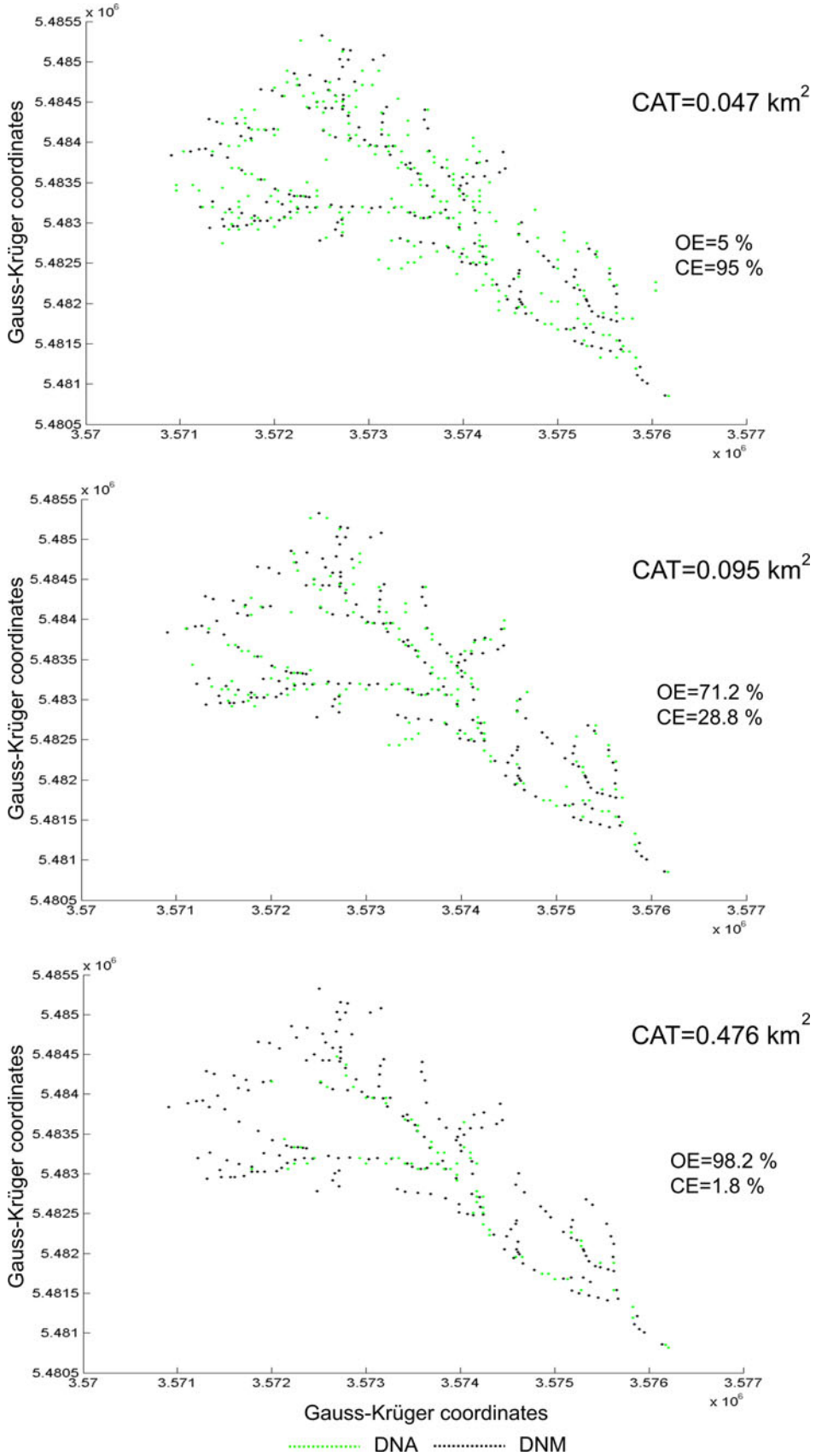


**Fig. 4** Effects (errors) of the DNA at different CAT's for a drainage network located in the North of the study area

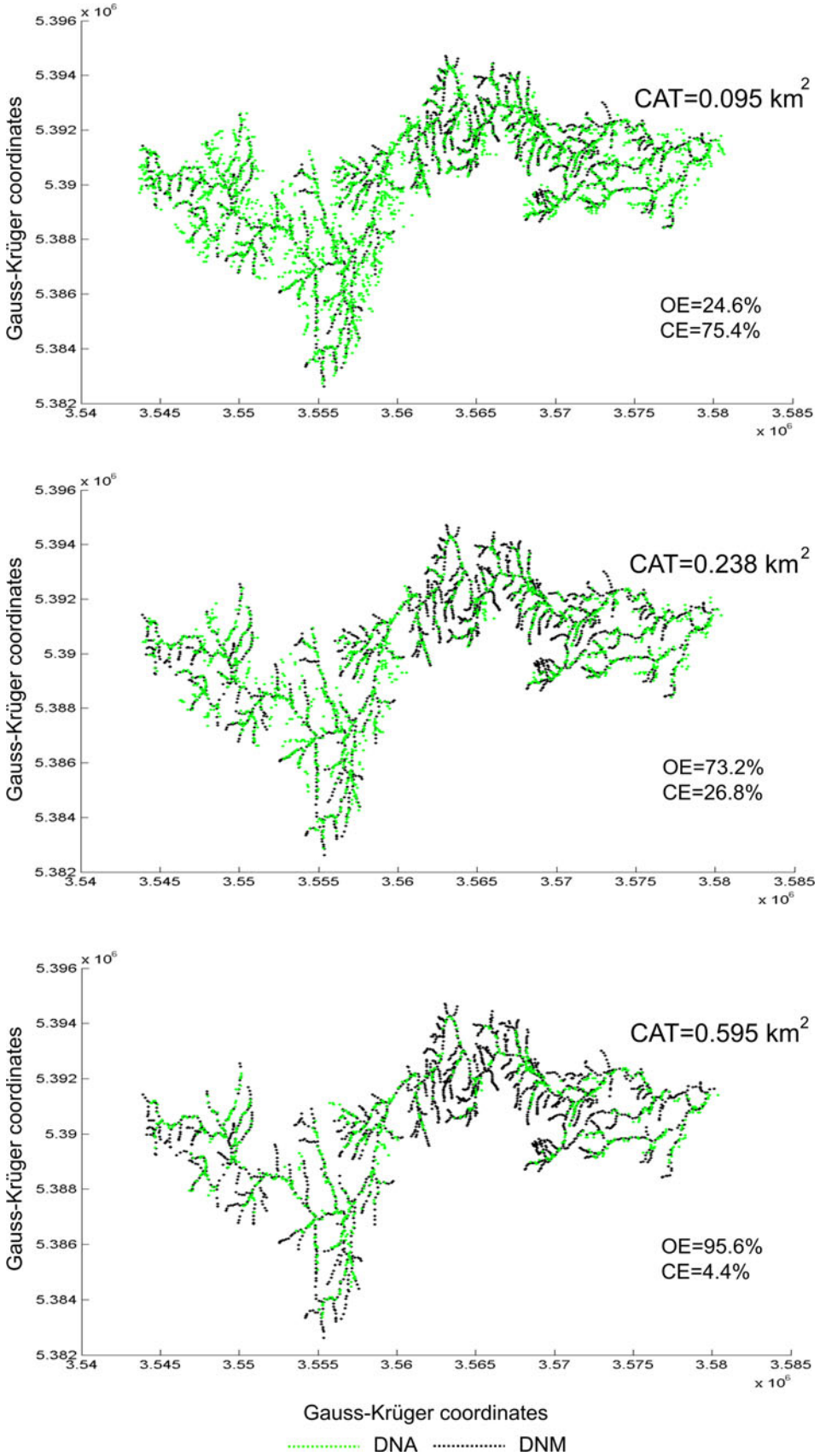


**Fig. 5** Effects (errors) of the DNA at different CAT's for a drainage network located in the South of the study area

unconsolidated deposits of recent age (score = 1). The different geological units (Appendix) were grouped into these four types according to the analysis of available literature data (Busteros et al. 1998; Franchi et al. 1998; Martínez et al. 2001) (Table 2, Appendix). Finally, the lithology (L) variable for each basin was obtained as:

$$L = \frac{\sum A_e \cdot S_e}{100} \quad (5)$$

where $A_e$ is the portion of the basin (%) belonging to a given rock-type erodibility and $S_e$ is the value score of the corresponding rock-type erodibility.

Fractal dimension (FD) describes the complexity of nature's shapes (Mandelbrot 1977) and characterizes the scaling properties of an object. Application to drainage networks contributes to the understanding of their maturity and ability to fill a plane (Dombrádi et al. 2007). In this work, we used the box-counting method, in which the object (i.e., drainage network) is cover with a regular grid of size r and one simply counts the number of grid boxes (Nr) that include part of the object (Rodriguez-Iturbe and Rinaldo 1997). The size of the boxes is successively reduced; plotting the logarithmic relationship between Nr and r and by measuring its slope, the FD is obtained.

The entire statistical analysis was carried out using the open source GNU Octave software. Variables not following a normal distribution were log-transformed (base 10) prior to analysis. For evaluation of normality of distribution, the Kolmogorov-Smirnov (K-S) statistical test was applied (Table 1). Since the variables display different nature (i.e., scale and measurement units), they were standardized by means of z-scores as follows:

$$Z_i = \frac{x_i - \mu}{SD} \quad (6)$$

where $z_i$ is the standard score of the sample i, $x_i$ the value of sample i, μ the mean and SD the standard deviation.

**Tabl 3** Geomorphometric data of 35 drainage basins. The basins number 8, 25 and 35 are named Fuerte Argentino, Salado and Verde, respectively

| Basin number | A km$^2$ | C | S (°) | $S_{sd}$ (°) | H (m) | $H_{sd}$ (m) | R | $R_n$ | L | U | D (km km$^{-2}$) | F | B | T | Sin | FD (-) |
|---|---|---|---|---|---|---|---|---|---|---|---|---|---|---|---|---|
| 1 | 11.7 | 1.74 | 1.91 | 1.0 | 70.1 | 29.6 | 0.025 | 0.373 | 0.87 | 3 | 2.41 | 3.16 | 5.57 | 2.48 | 1.06 | 1.35 |
| 2 | 68.6 | 1.67 | 1.62 | 0.9 | 113.6 | 40.0 | 0.013 | 0.402 | 0.87 | 5 | 2.35 | 2.81 | 3.75 | 2.14 | 1.25 | 1.47 |
| 3 | 11.9 | 2.00 | 1.87 | 1.1 | 96.9 | 46.8 | 0.023 | 0.476 | 0.93 | 4 | 2.82 | 3.62 | 3.18 | 2.61 | 1.14 | 1.40 |
| 4 | 22.3 | 1.75 | 1.79 | 1.1 | 99.6 | 46.9 | 0.019 | 0.419 | 0.86 | 4 | 2.48 | 2.69 | 3.59 | 2.02 | 1.27 | 1.40 |
| 5 | 19.0 | 1.90 | 1.62 | 0.9 | 96.8 | 46.8 | 0.018 | 0.391 | 0.86 | 3 | 2.35 | 2.58 | 6.90 | 2.00 | 1.19 | 1.40 |
| 6 | 16.1 | 2.01 | 2.11 | 1.2 | 85.6 | 36.3 | 0.018 | 0.389 | 0.91 | 4 | 2.49 | 3.73 | 3.90 | 2.92 | 1.17 | 1.41 |
| 7 | 22.4 | 1.89 | 1.95 | 1.8 | 71.8 | 31.6 | 0.016 | 0.375 | 0.96 | 5 | 2.71 | 3.76 | 2.89 | 2.73 | 1.30 | 1.42 |
| 8 | 773.1 | 2.98 | 1.06 | 1.4 | 262.3 | 110.2 | 0.007 | 1.032 | 0.78 | 6 | 1.87 | 1.54 | 4.12 | 1.20 | 1.41 | 1.66 |
| 9 | 21.7 | 1.81 | 2.14 | 2.5 | 68.1 | 42.4 | 0.016 | 0.296 | 0.93 | 4 | 2.10 | 2.40 | 3.71 | 1.89 | 1.12 | 1.33 |
| 10 | 11.2 | 1.97 | 1.70 | 2.2 | 42.6 | 30.9 | 0.019 | 0.318 | 0.96 | 3 | 2.30 | 2.23 | 4.50 | 1.78 | 1.12 | 1.28 |
| 11 | 25.6 | 1.71 | 1.56 | 2.5 | 74.7 | 45.0 | 0.014 | 0.307 | 0.96 | 4 | 2.10 | 2.15 | 3.73 | 1.64 | 1.19 | 1.35 |
| 12 | 84.7 | 3.26 | 1.06 | 1.1 | 156.6 | 54.2 | 0.007 | 0.440 | 0.96 | 4 | 1.89 | 1.71 | 5.24 | 1.42 | 1.33 | 1.35 |
| 13 | 38.1 | 2.20 | 1.36 | 1.1 | 136.6 | 45.2 | 0.011 | 0.319 | 0.96 | 4 | 1.69 | 1.63 | 4.02 | 1.31 | 1.11 | 1.29 |
| 14 | 31.2 | 2.24 | 1.73 | 1.7 | 120.7 | 52.8 | 0.012 | 0.342 | 0.94 | 4 | 1.89 | 1.89 | 3.91 | 1.51 | 1.22 | 1.30 |
| 15 | 12.5 | 2.09 | 2.05 | 1.3 | 98.3 | 46.1 | 0.018 | 0.311 | 0.95 | 3 | 1.86 | 2.01 | 4.50 | 1.60 | 1.05 | 1.24 |
| 16 | 13.8 | 1.32 | 2.11 | 1.7 | 67.7 | 39.1 | 0.024 | 0.311 | 0.94 | 3 | 2.01 | 2.11 | 5.00 | 1.75 | 1.26 | 1.29 |
| 17 | 181.2 | 2.48 | 1.16 | 0.9 | 168.2 | 53.6 | 0.007 | 0.491 | 0.96 | 5 | 1.93 | 1.91 | 4.42 | 1.56 | 1.11 | 1.46 |
| 18 | 12.2 | 1.86 | 1.41 | 0.8 | 60.7 | 32.3 | 0.021 | 0.307 | 0.97 | 3 | 2.06 | 1.97 | 4.30 | 1.48 | 1.12 | 1.25 |
| 19 | 10.0 | 1.88 | 1.37 | 0.6 | 59.1 | 38.1 | 0.022 | 0.376 | 1.00 | 3 | 2.41 | 2.09 | 4.00 | 1.59 | 0.99 | 1.28 |
| 20 | 183.0 | 2.03 | 1.16 | 0.9 | 159.4 | 58.7 | 0.007 | 0.477 | 0.92 | 5 | 1.90 | 1.97 | 4.18 | 1.55 | 1.20 | 1.55 |
| 21 | 30.9 | 2.41 | 1.08 | 0.8 | 114.1 | 59.0 | 0.012 | 0.466 | 0.93 | 4 | 2.43 | 2.59 | 4.57 | 2.17 | 1.21 | 1.39 |
| 22 | 55.8 | 2.06 | 1.66 | 1.7 | 77.1 | 37.9 | 0.014 | 0.499 | 0.93 | 5 | 2.81 | 4.21 | 3.79 | 3.26 | 1.29 | 1.48 |
| 23 | 15.4 | 1.67 | 2.38 | 2.0 | 60.2 | 38.7 | 0.022 | 0.396 | 0.78 | 4 | 2.54 | 3.44 | 3.69 | 2.66 | 1.13 | 1.40 |
| 24 | 23.9 | 1.64 | 1.20 | 1.1 | 47.4 | 20.7 | 0.015 | 0.365 | 0.88 | 4 | 2.64 | 3.35 | 4.02 | 2.56 | 1.06 | 1.46 |
| 25 | 4090.8 | 2.06 | 2.23 | 2.5 | 565.3 | 331.7 | 0.010 | 2.497 | 0.20 | 7 | 1.52 | 1.10 | 4.14 | 0.86 | 1.46 | 1.77 |
| 26 | 318.9 | 2.39 | 1.82 | 1.7 | 241.5 | 85.5 | 0.012 | 0.726 | 0.50 | 5 | 1.59 | 1.24 | 4.61 | 0.98 | 1.30 | 1.43 |
| 27 | 137.2 | 2.18 | 2.16 | 1.7 | 169.5 | 79.1 | 0.013 | 0.536 | 0.16 | 5 | 1.52 | 1.17 | 3.47 | 0.87 | 1.26 | 1.41 |
| 28 | 91.0 | 1.85 | 1.45 | 1.1 | 124.5 | 62.0 | 0.014 | 0.514 | 0.50 | 4 | 1.72 | 1.07 | 4.29 | 0.85 | 1.23 | 1.41 |
| 29 | 156.5 | 2.27 | 1.66 | 1.3 | 145.7 | 100.7 | 0.012 | 0.553 | 0.31 | 5 | 1.57 | 1.06 | 3.56 | 0.82 | 1.17 | 1.41 |
| 30 | 90.1 | 1.92 | 1.52 | 0.8 | 111.6 | 59.0 | 0.012 | 0.370 | 0.09 | 4 | 1.52 | 1.08 | 4.44 | 0.88 | 1.19 | 1.37 |
| 31 | 19.2 | 2.30 | 1.38 | 0.8 | 77.0 | 31.1 | 0.013 | 0.225 | 0.30 | 3 | 1.50 | 1.20 | 4.67 | 0.99 | 1.14 | 1.26 |
| 32 | 85.9 | 2.61 | 1.59 | 0.9 | 169.1 | 65.2 | 0.013 | 0.471 | 0.15 | 4 | 1.49 | 0.91 | 4.13 | 0.73 | 1.10 | 1.39 |
| 33 | 119.4 | 1.94 | 1.60 | 1.1 | 156.0 | 59.7 | 0.012 | 0.466 | 0.28 | 5 | 1.56 | 1.28 | 3.48 | 0.97 | 1.20 | 1.44 |
| 34 | 13.2 | 1.58 | 1.25 | 0.6 | 40.7 | 16.9 | 0.012 | 0.107 | 0.20 | 3 | 1.35 | 1.44 | 4.00 | 1.14 | 1.00 | 1.24 |
| 35 | 2343.1 | 3.74 | 2.59 | 2.7 | 600.8 | 334.8 | 0.010 | 2.450 | 0.27 | 6 | 1.51 | 0.99 | 4.65 | 0.78 | 1.38 | 1.62 |
| Mean | 261.8 | 2.1 | 1.7 | 1.4 | 137.4 | 66.0 | 0.015 | 0.54 | 0.71 | 4.2 | 2.0 | 2.1 | 4.2 | 1.6 | 1.2 | 1.4 |
| SD | 780.2 | 0.5 | 0.4 | 0.6 | 122.9 | 69.7 | 0.005 | 0.51 | 0.32 | 1.0 | 0.4 | 0.9 | 0.7 | 0.7 | 0.1 | 0.1 |

Initially, a correlation analysis was performed by Pearson product–moment, which measures the strength of a linear relationship between two variables. The level of significance was set at $P = 0.05$. Multivariate techniques were used in order to assess the association among all variables (PCA) of the selected drainage systems and to group them by homogeneous attributes (PCA and CA). PCA is based on the diagonalization of the correlation matrix allowing the transformation of correlated variables into orthogonal variables called principal components, making it easier to interpret a given multidimensional space. CA was performed to define groups (or clusters) of objects (i.e., drainage basins) on the basis of their geomorphometry. Drainage basins were hierarchically clustered by using Ward's method (linkage rule) and Euclidean distance (similarity measure). Ward's method and the Euclidean distance were chosen to allow comparing the results from CA with those of PCA.

## Results and discussion

### Drainage network adjustment results

A set of CAT's were tested for each lithological environment (North and South from the Salado System) through the comparison of DNA and DNM. The errors ($E_t$) of the DNA at different CAT's followed a trend that was similar to an inverted Gaussian curve in both environments and at varying scales, in which the adequate CAT could be clearly observed (Fig. 3). The adequate CAT's were nearly 0.095 $km^2$ with an $E_t$ of 0.04 ($k \times l = 9 \times 9$) (Fig. 3a) and close to 0.25 $km^2$ with an $E_t$ of 0.06 ($k \times l = 9 \times 9$) (Fig. 3b), for the North and South parts of the study area, respectively. In addition, by testing both $9 \times 9$ and $15 \times 15$ window dimensions, the adequate CAT's were the same. The errors ($E_t$) belonging to the window of dimension $9 \times 9$ resulted in lower values.

The omission and commission errors of the DNA at different CAT's followed an inverted trend between them in all the cases (Fig. 3). When the CAT rises, omission and commission errors increase and decrease, respectively. According to the optimal CAT for each environment, distribution of both omission and commission errors was 71.2 and 28.8 % (North part), and 73.2 and 26.2 % (South part), respectively (Figs. 4 and 5).

### Statistical geomorphometric analysis

The behavior of certain variables, such as the case of area, elevation and ruggedness number had showed significant differences throughout the studied drainage basins (Table 3). This can be clearly observed in the standard deviation values. An important aspect of this high variability is the occurrence of many complex geological processes that affected the whole study area in the past, providing the actual geomorphologic structure (Genchi 2012).

Pearson product–moment correlation analysis between the considered variables is reported in Table 4. Most of the correlations are statistically significant at the 0.05 level, with the exception of slope (S and $S_{sd}$) and mean bifurcation ratio, which showed no significance in almost all their relationships. Some pairs of variables are very highly correlated to each

**Table 4** Pearson product–moment correlation coefficients

| | A | C | S | $S_{sd}$ | H | $H_{sd}$ | R | $R_n$ | L | U | D | F | B | T | Sin | FD |
|---|---|---|---|---|---|---|---|---|---|---|---|---|---|---|---|---|
| A | 1.00 | | | | | | | | | | | | | | | |
| C | 0.61* | 1.00 | | | | | | | | | | | | | | |
| S | 0.09 | −0.07 | 1.00 | | | | | | | | | | | | | |
| $S_{sd}$ | 0.33 | 0.14 | 0.67* | 1.00 | | | | | | | | | | | | |
| H | 0.92* | 0.69* | 0.18 | 0.27 | 1.00 | | | | | | | | | | | |
| $H_{sd}$ | 0.89* | 0.62* | 0.33 | 0.45* | 0.94* | 1.00 | | | | | | | | | | |
| R | −0.72* | −0.60* | 0.43* | 0.02 | −0.62* | −0.46* | 1.00 | | | | | | | | | |
| $R_n$ | 0.85* | 0.58* | 0.34* | 0.45* | 0.87* | 0.92* | −0.34* | 1.00 | | | | | | | | |
| L | −0.51* | −0.21 | −0.17 | −0.02 | −0.43* | −0.45* | 0.35* | −0.27 | 1.00 | | | | | | | |
| U | 0.89* | 0.44* | 0.17 | 0.41* | 0.79* | 0.76* | −0.62* | 0.81* | −0.32 | 1.00 | | | | | | |
| D | −0.53* | −0.36* | 0.05 | −0.02 | −0.51* | −0.46* | 0.56* | −0.16 | 0.74* | −0.21 | 1.00 | | | | | |
| F | −0.54* | −0.40* | 0.14 | 0.00 | −0.53* | −0.52* | 0.52* | −0.24 | 0.67* | −0.19 | 0.95* | 1.00 | | | | |
| B | −0.03 | 0.17 | −0.14 | −0.18 | 0.05 | 0.02 | 0.07 | 0.01 | 0.07 | −0.36* | −0.11 | −0.16 | 1.00 | | | |
| T | −0.54* | −0.39* | 0.12 | −0.00 | −0.54* | −0.53* | 0.50* | −0.25 | 0.69* | −0.21 | 0.94* | 0.99* | −0.11 | 1.00 | | |
| Sin | 0.72* | 0.44* | 0.22 | 0.47* | 0.70* | 0.70* | −0.42* | 0.73* | −0.19 | 0.75* | −0.14 | −0.16 | −0.02 | −0.16 | 1.00 | |
| FD | 0.84* | 0.37* | 0.14 | 0.32 | 0.74* | 0.72* | −0.47* | 0.86* | −0.25 | 0.90* | −0.06 | −0.06 | −0.10 | −0.08 | 0.72* | 1.00 |

* Significant correlations at $P < 0.05$

other due to various causes, including, for instance, obvious correlations between variables (e.g., A and U –$r^2$ = 0.89-, D and F –$r^2$ = 0.95-) or variables that are derivative of others (e.g., F and T -$r^2$ = 0.99-).

In this work, we carried out a multivariate analysis following two ways: (1) by considering all the drainage basins with the exception of basins number 25 (Salado Basin) and 35 (Verde Basin) (33 cases -33C-) (Fig. 6, Table 5), and (2) by considering all the drainage basins (35 cases -35C-) (Fig. 7, Table 5). This is due to the fact that the Salado and Verde drainage basins are the largest hydrographic systems by 2–4 orders of magnitude and they may well give a bias in the distribution on the axial plane. Regarding the PCA analysis, the first four principal components (PC's) axes were considered to be statistically significant, that is, PC with eigenvalues greater than one; they explain 83.7 and 86.9 % of the total variance for the 33C and 35C scenarios, respectively (Table 5). All the communalities of variables employed in the PCA are presented in Table 5. The communalities were above of 0.63 for both scenarios, which means that the variance can be explained by the extracted PC at >63 %.

The PC1, which explains 42.2 (33C) and 48.9 % (35C) of the total variance, is clearly correlated to dimension and relief variables (Table 5). This PC showed a high negative correlation with area, compactness index, elevation (H and $H_{sd}$), ruggedness number and network order, and a high positive correlation with relief ratio. Sinuosity factor reached a considerable value (-0.76) for 35C but not for 33C (-0.58). In the particular cases of fractal dimension and lithology, their maximum factor loadings for 33C corresponded to PC2 while for 35C they corresponded to PC1. Therefore, taking into account these latter variables, drainage basins number 25 and 35 have had a certain influence on the multivariate analysis. Considering both scenarios (33C and 35C), the above-

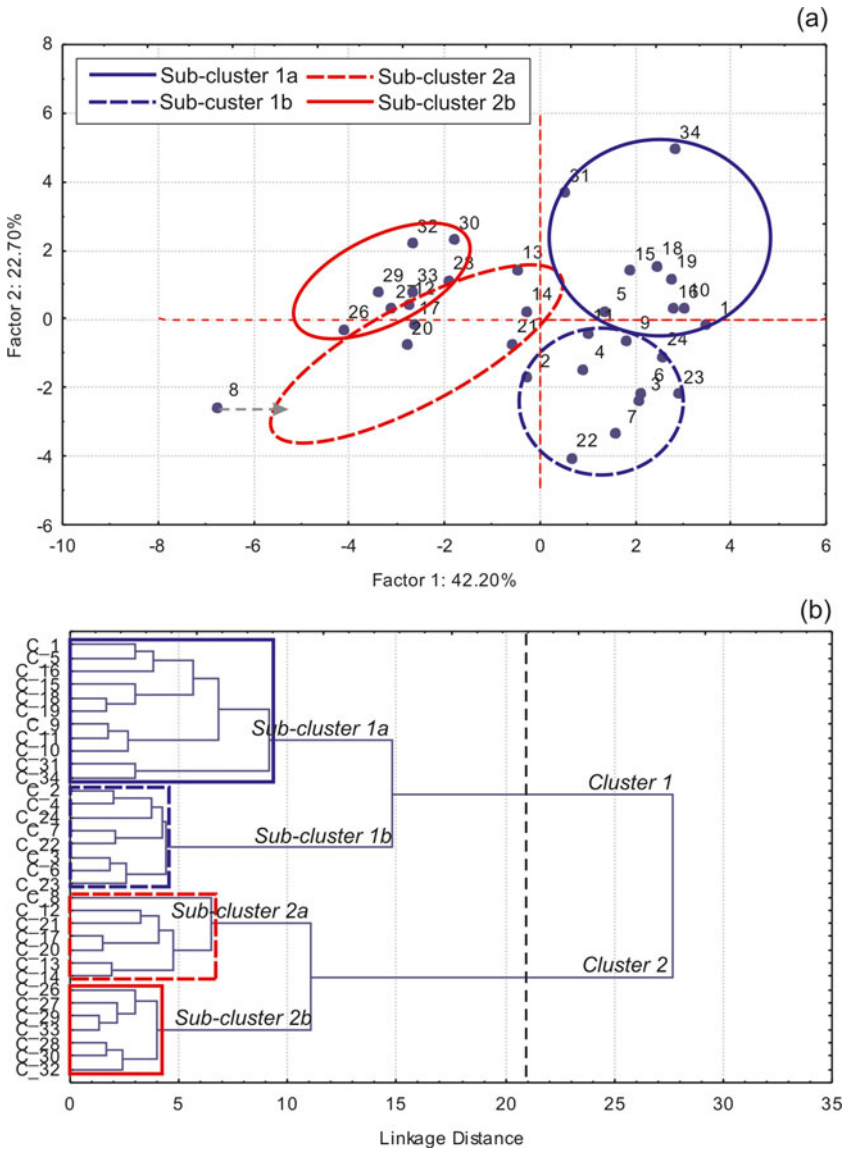


**Fig. 6** PCA (**a**) and CA (**b**) showing clustering of 33 drainage basins. The dark dashed line (**b**) displays the cut on the maximum difference between distances

**Table 5** Results of the principal component analysis (33C: 33 cases, 35C: 35 cases

| | PC1 | | PC2 | | PC3 | | PC4 | | Communalities | |
|---|---|---|---|---|---|---|---|---|---|---|
| | 33C | 35C | 33C | 35C | 33C | 35C | 33C | 35C | 33C | 35C |
| A | **−0.964** | **−0.977** | −0.115 | −0.058 | 0.009 | −0.108 | 0.090 | −0.043 | 0.951 | 0.972 |
| C | **−0.706** | **−0.674** | 0.003 | 0.082 | −0.319 | −0.278 | −0.225 | 0.313 | 0.650 | 0.636 |
| S | 0.388 | −0.157 | −0.272 | −0.498 | **0.765** | **0.799** | −0.253 | 0.099 | 0.874 | 0.921 |
| $S_{sd}$ | 0.109 | −0.371 | −0.399 | −0.521 | **0.655** | **0.530** | −0.183 | 0.035 | 0.634 | 0.691 |
| H | **−0.921** | **−0.952** | −0.093 | −0.055 | −0.002 | −0.063 | −0.192 | 0.127 | 0.895 | 0.929 |
| $H_{sd}$ | **−0.852** | **−0.935** | −0.136 | −0.144 | 0.217 | 0.133 | −0.320 | 0.155 | 0.895 | 0.937 |
| R | **0.796** | **0.690** | −0.124 | −0.292 | 0.248 | 0.489 | −0.330 | 0.234 | 0.819 | 0.855 |
| $R_n$ | **−0.686** | **−0.848** | −0.564 | −0.410 | −0.009 | −0.006 | −0.269 | 0.184 | 0.861 | 0.922 |
| L | 0.420 | **0.567** | **−0.552** | −0.453 | −0.377 | −0.374 | −0.248 | 0.250 | 0.685 | 0.730 |
| U | **−0.747** | **−0.839** | −0.536 | −0.388 | 0.122 | −0.163 | 0.342 | −0.312 | 0.976 | 0.979 |
| D | 0.561 | 0.604 | **−0.762** | **−0.723** | −0.245 | −0.255 | −0.018 | 0.064 | 0.956 | 0.956 |
| F | 0.596 | 0.617 | **−0.752** | **−0.732** | −0.176 | −0.206 | 0.095 | −0.026 | 0.960 | 0.959 |
| B | 0.066 | 0.024 | 0.298 | 0.264 | −0.469 | −0.108 | **−0.703** | **0.894** | 0.807 | 0.880 |
| T | 0.600 | 0.625 | **−0.738** | **−0.716** | −0.204 | −0.221 | 0.063 | 0.014 | 0.950 | 0.952 |
| Sin | **−0.585** | **−0.735** | −0.504 | −0.406 | 0.098 | −0.088 | −0.194 | 0.082 | 0.643 | 0.719 |
| FD | −0.610 | **−0.760** | **−0.634** | −0.468 | −0.162 | −0.241 | 0.194 | −0.081 | 0.838 | 0.861 |
| EV | 6.75 | 7.83 | 3.63 | 3.18 | 1.77 | 1.67 | 1.24 | 1.22 | | |
| Var (%) | 42.20 | 48.92 | 22.70 | 19.92 | 11.07 | 10.43 | 7.74 | 7.60 | | |
| CVa (%) | 42.20 | 48.92 | 64.90 | 68.83 | 75.97 | 79.27 | 83.71 | 86.87 | | |

*EV* Eigenvalue, *Va* Variance, *CVa* Cumulative Variance). Maximum factor loading for each variable is shown in bold

mentioned variables (except fractal dimension and lithology) exhibited similar factor loadings, with small differences ranging from 0.7 % (A) to 8.1 % ($R_n$) (Table 5).

The second PC contributes 22.7 (33C) and 19.9 % (35C) of the total variance. It is mainly determined by the drainage network properties (Table 5). The PC2 showed a high (negative) association with drainage density, drainage frequency and torrentiality coefficient. Taking into consideration both scenarios (33C and 35C), these variables showed very similar factor loadings. PC3 explains 11 (33C) and 10.4 % (35C) of the total variance, with an eigenvalue close to 2. The variables that correspond to the PC3 are those relative to the slope (S and $S_{sd}$), being more accentuated for mean slope (-0.75 -33 and -0.79 -35C-). Finally, the only variable associated to PC4 is mean bifurcation ratio with a factor loading of -0.70 (33C) and 0.89 (35C).

In general terms, from the comparison of PCA and CA analysis (drainage basins) (Figs. 6 and 7), we found that the first drainage basins space (i.e., PC1-PC2) allows a good understanding of the clustering from the CA, whatever the scenario (33 or 35C). The clustering results can be further reworked by cutting the dendrogram at different levels. Two main clusters (cluster 1 and cluster 2) can be distinguished based on the detection of region with greatest separation (Figs. 6b and 7b). Final clusters were chosen by cutting the dendrogram at a successive level of the hierarchy, that is, two sub-clusters: 1a and 1b, and 2a and 2b (Figs. 6b and 7b).

The linkage distance between the clusters 1 and 2 was longer for 35C than for 33C, as was expected (Figs. 6b and 7b). The cluster 1 showed identical behavior in both scenarios (33 and 35C), while cluster 2 presented a noticeable difference; by adding the two large drainage basins (25 and 35), it is lead to a re-clustering of the basins, with greater differences among the sub-clusters (Figs. 6 and 7).

The drainage basins within each cluster are mostly located adjacent to one another, showing strong spatial continuity (Figs. 1, 6 and 7). Almost all of the basins of the sub-clusters 1a and 1b are located nearly exclusively within the North part of the study area, with the exception of basins number 31 and 34; the sub-cluster 2a, for the case of 33C, also contains basins that are located within the North part. Regarding the remaining drainage basins which were included in the sub-cluster 2b, they are located entirely in the South part for the case of 33C, while for the 35C, the basins occupy both parts almost equally (46 % -North- and 6 4 % -South-) due to the fact that the sub-cluster 2a grouped only three basins.

The mean and standard deviation of the analyzed variables were calculated for each sub-cluster (Table 6). Cluster 1 is characterized by small size and elongated drainage basins, which are located on terrain exhibiting low mean elevation,

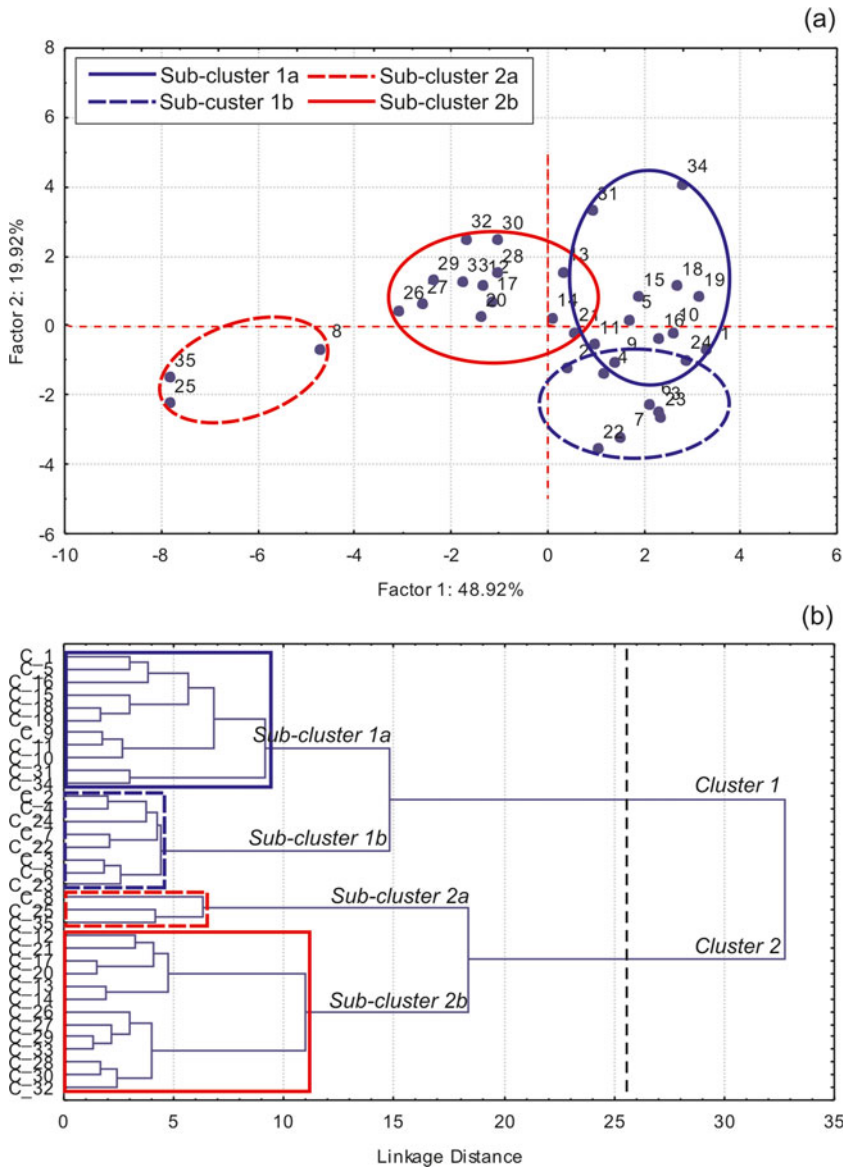


**Fig. 7** PCA (**a**) and CA (**b**) showing clustering of 35 drainage basins. The dark dashed line (**b**) displays the cut on the region with greater separation

low ruggedness number and high erodibility (lithology variable). Basins in cluster 1 show in average low to moderate values of drainage density (2–2.6 km km$^{-1}$) and low to moderate values of torrentiality coefficient (1.6–2.6) (Table 6). The major differences between sub-clusters 1a and 1b were found in network order (sub-cluster 1a: 3.4, sub-cluster 1b: 4.4, i.e., 26.6 %), drainage density (sub-cluster 1a: 2 km km$^{-1}$; sub-cluster 1b: 2.6 km km$^{-1}$, i.e., 26.5 %), drainage frequency (sub-cluster 1a: 2, sub-cluster 1b: 3.5, i.e., 67.5 %) and torrentiality coefficient (sub-cluster 1a: 1.6; sub-cluster 1b: 2.6, i.e., 61.8 %) (Table 6). Therefore, the latter key characteristics allow to expect that drainage basins within sub-cluster 1b have a fast hydrological response to precipitation events.

Cluster 2 is characterized by medium to large drainage basins that have very elongated shapes (Table 6). These basins are located on terrains with mean elevation ranging (in average) from 160 (sub-clusters 2a and 2d -33C-) to 476 m (sub-cluster 2a -35C-). The terrain exhibits moderate to high ruggedness number, being more noticeable in the case of sub-cluster 2a -35C-; this reflects the structural complexity of the terrain that is associated with a relatively high relief. Concerning drainage network, it was found that the density (and also frequency) is low, with values lesser than 2 (Table 6). The latter is indicating that the terrain is covered by resistant rocks, such as was found in the low level of erodibility, with the exception of the sub-cluster 2a -33C- (Table 6). The torrentiality coefficient is also low, as was expected. Therefore, the above characteristics suggest that the drainage basins in cluster 2 have generally a slow hydrological response.

Differences in lithology of the terrain imply an important aspect in the physiography and fluvial landscape

**Table 6** Statistic of the geomorphometric properties for each sub-cluster (*SD* standard deviation)

| Variable | Sub-cluster 1a | | Sub-cluster 1b | | Sub-cluster 2a | | | | Sub-cluster 2b | | | |
|---|---|---|---|---|---|---|---|---|---|---|---|---|
| | | | | | 33C | | 35C | | 33C | | 35C | |
| | Mean | SD | Mean | SD | Mean | SD | Mean | SD | Mean | SD | Mean | SD |
| A ($km^2$) | 34.5 | 45.9 | 29.5 | 20.8 | 188.9 | 266.1 | 2402.3 | 1659.6 | 142.7 | 82.1 | 119.1 | 79.4 |
| C | 1.92 | 0.33 | 1.84 | 0.17 | 2.51 | 0.45 | 2.93 | 0.84 | 2.17 | 0.28 | 2.29 | 0.37 |
| S (°) | 1.74 | 0.27 | 1.82 | 0.35 | 1.23 | 0.24 | 1.96 | 0.80 | 1.69 | 0.24 | 1.49 | 0.32 |
| Ssd (°) | 1.43 | 0.69 | 1.36 | 0.41 | 1.13 | 0.32 | 2.20 | 0.70 | 1.23 | 0.36 | 1.16 | 0.34 |
| H (m) | 86.6 | 38.7 | 81.5 | 21.8 | 159.7 | 49.6 | 476.1 | 186.0 | 159.7 | 42.1 | 151.8 | 34.2 |
| Hsd (m) | 46.9 | 20.4 | 37.4 | 8.5 | 62.0 | 21.8 | 258.9 | 128.8 | 73.0 | 15.9 | 64.2 | 15.3 |
| R | 0.02 | 0.00 | 0.02 | 0.00 | 0.01 | 0.00 | 0.01 | 0.00 | 0.01 | 0.00 | 0.01 | 0.00 |
| Rn | 0.36 | 0.08 | 0.42 | 0.05 | 0.51 | 0.24 | 1.99 | 0.83 | 0.52 | 0.11 | 0.47 | 0.10 |
| L | 0.81 | 0.29 | 0.89 | 0.06 | 0.92 | 0.06 | 0.42 | 0.32 | 0.28 | 0.17 | 0.59 | 0.36 |
| U | 3.45 | 0.69 | 4.38 | 0.52 | 4.57 | 0.79 | 6.33 | 0.58 | 4.57 | 0.53 | 4.46 | 0.52 |
| D (km $km^{-2}$) | 2.06 | 0.32 | 2.61 | 0.17 | 1.94 | 0.23 | 1.63 | 0.21 | 1.57 | 0.08 | 1.75 | 0.26 |
| F | 2.06 | 0.63 | 3.45 | 0.50 | 1.89 | 0.35 | 1.21 | 0.29 | 1.12 | 0.13 | 1.50 | 0.49 |
| B | 4.54 | 0.98 | 3.60 | 0.38 | 4.35 | 0.45 | 4.30 | 0.30 | 4.00 | 0.49 | 4.18 | 0.51 |
| T | 1.61 | 0.50 | 2.61 | 0.40 | 1.53 | 0.31 | 0.95 | 0.22 | 0.87 | 0.09 | 1.20 | 0.42 |
| Sin | 1.12 | 0.08 | 1.20 | 0.09 | 1.23 | 0.11 | 1.42 | 0.04 | 1.21 | 0.06 | 1.20 | 0.07 |
| FD (-) | 1.32 | 0.06 | 1.43 | 0.03 | 1.43 | 0.14 | 1.68 | 0.08 | 1.41 | 0.02 | 1.40 | 0.07 |

characterization. The above analysis indicates that the association of the geomorphometric variables tends to be consistent with the lithology, similar to that found in prior studies (Miller et al. 1990; Subyani et al. 2010). In fact, the Salado Basin, which divides the region into two parts from a geological point of view, it also divides the two main clusters (cluster 1 and cluster 2) with a few exceptions. The drainage systems included within a given cluster (i.e., cluster 1 and cluster 2) might have evolved in a similar way.

## Conclusions

The automated extraction of drainage network from DEM using geospatial tools in GIS is faster, more objective, and consistent than manual techniques. However, like any automated tool, it requires setting certain parameters such as the CAT. In the first stage of the study, an adequate threshold was determined for two clearly different lithological environments from comparing automated and manual drainage networks. The lithology shows a greater variability as compared to climate, vegetation or land use. The study showed that it was possible to derive automated drainage networks from DEM with errors ($E_t$) lower than 6 %.

Geomorphometric analysis provides a quantitative physical description of fluvial landforms, which is able to explain and predict potential hydrologic effects. Geomorphometric data of 35 drainage basins were statically analyzed using bivariate and multivariate techniques. Regarding groups of geomorphometric properties, the first principal component, which explains 42.2 (33C) and 48.9 % (35C) of the total variance, is correlated to dimension and relief variables; the second PC, which contributes 22.7 (33C) and 19.9 % (35C) of the total variance, is mainly determined by the drainage network properties; the third PC, which explains 11 (33C) and 10.4 % (35C) of the total variance, is correlated to slope. In the case of the lithology, the factor loading is around 0.5 for the first two principal components, indicating an appreciable association with the main variables considered. By comparing PCA and CA, it was found that the former allows a good understanding of the clustering of basins from the CA. All basins were clustered into 4 groups following a strong spatial continuity, showing a consistent association of the geomorphometric properties with the lithology. From the hydrological point of view, results suggest that sub-cluster 1b is the only one that contains basins with a faster hydrological response.

The studied drainage systems are, with few exceptions, ephemeral, carrying water during and soon after intense precipitation events. Although extreme precipitation events are exceptional, the historical maximum values (102 and 120 mm in a 24-h period) reveal potential flood risks. The potential increase in the number of these extreme events in the future due to climate change may lead to more disturbances that have to be taken into account in the field of spatial planning. In this sense, the large amount of data generated

herein may serve as the input for rainfall-runoff models. Finally, the proposed methodology, including determination of adequate CAT and statistical treatment of the drainage basins, could be applied elsewhere. *PCA* Principal Component Analysis, *CA* Cluster Analysis, *DEM* Digital Elevation Model, *SRTM* Shuttle Radar Topographic Mission, *GIS* Geographic Information System, *CAT* Contributing Area Threshold, *DNA* Drainage Network Automatically Extracted, *DNM* Drainage Network Manually Delineated, *PC* Principal Component.

**Acknowledgments** Partial support of this work was provided by grants from Consejo Nacional de Investigaciones Científicas y Técnicas (CONICET), Agencia Nacional de Promoción Científica y Tecnológica (PICT 2012-1065), and Universidad Nacional del Sur (PGI 24/H127).

**Compliance with ethical standards**

**Conflict of interest** The authors declare that they have no conflict of interest.

## References

Al Rawashdeh SB (2012) Assessment of extraction drainage pattern from topographic maps based on photogrammetry. Arab J Geosci 6(12): 4873–4880. doi:10.1007/s12517-012-0718-z

Ali GA, Roy AG, Turme MC, Courchesne F (2010) Multivariate analysis as a tool to infer hydrologic response types and controlling variables in a humid temperate catchment. Hydrol Process 24:2912–2923. doi:10.1002/hyp.7705

Bali R, Agarwal KK, Nawaz Ali S, Rastogi SK, Krishna K (2011) Drainage morphometry of Himalayan Glacio-fluvial basin, India: hydrologic and neotectonic implications. Environ Earth Sci 66: 1163–1174. doi:10.1007/s12665-011-1324-1

Busteros A, Giacosa R, Lema H, Zubia M (1998) Descripción de la Hoja Geológica Hoja 4166-IV- Sierra Grande, Provincia de Río Negro. SEGEMAR, Buenos Aires

Cabrera A (1976) Regiones fitogeográficas argentinas. In: Kugler W (ed) Enciclopedia Argentina de Agricultura y Jardinería, 2nd edn. Acme, Buenos Aires, pp 1–85

Charon JE (1974) Hydrogeological applications of ERTS satellite imagery. In: Proc UN/FAO regional seminar on remote sensing of earth resources and environment. Commonwealth Science Council, Cairo, pp 439–456

Chen C, Yu F (2011) Morphometric analysis of debris flows and their source areas using GIS. Geomorphology 29(3-4):387–397. doi:10.1016/j.geomorph.2011.03.002

Coates DR (1958) Quantitative geomorphology of small drainage basins of southern Indiana (Tech. Rep. 10). Columbia University, New York

Dombrádi E, Timár G, Bada G, Cloetingh S, Horváth F (2007) Fractal dimension estimations of drainage network in the Carpathian–Pannonian system. Global Planet Change 58:197–213. doi:10.1016/j.gloplacha.2007.02.011

Ebisemiju FS (1976) Morphometric work with Nigerian topographical maps. Nigerian Geogr J 19:65–77

Ebisemiju FS (1979) An objective criterion for the selection of representative basins. Water Resour Res 15(1):148–158. doi:10.1029/WR015i001p00148

Franchi M, Remesal M, Ardolino A (1998) Descripción de la Hoja Geológica Hoja 4166-III- Cona Niyeu, Provincia de Río Negro. SEGEMAR, Buenos Aires

Gatziolis D, Fried JS (2004) Adding Gaussian noise to inaccurate digital elevation models improves spatial fidelity of derived drainage networks. Water Resour Res 40, W02508. doi:10.1029/2002WR001735

Genchi SA (2012) Geomorfología regional y dinámica costera del sector Occidental del golfo San Matías (Unpublished doctoral thesis). Universidad Nacional del Sur, Argentina

Genchi SA, Carbone ME, Piccolo MC, Perillo GME (2011) Clasificación geomorfológica automatizada en terrazas del noreste del Macizo Norpatagónico, Argentina. GeoFocus 11:182–206

Ghimire M (2014) Multivariate morphological characteristics and classification of first-order basins in the Siwaliks, Nepal. Geomorphology 204:192–207. doi:10.1016/j.geomorph.2013.08.004

Gómez-Villar A, Álvarez-Martínez J, García-Ruiz JM (2006) Factors influencing the presence or absence of tributary-junction fans in the Iberian Range, Spain. Geomorphology 81(3-4):252–264. doi:10.1016/j.geomorph.2006.04.011

González DEF, Malagnino EC (1984) Geomorfología. In: Ramos VA (ed) Relatorio del IX Congreso Geológico Argentino. Geología y recursos naturales de la Provincia de Río Negro Asociación Geológica Argentina, Buenos Aires, pp 347–364

Gravelius H (1914) Grundriß der Gesamten Gewässerkunde, Band 1: Flußkunde. Goschen, Berlin

Horton RE (1945) Erosional development of streams and their drainage basins; hydrophysical approach to quantitative morphology. Geol Soc Am Bull 56:275–370

Jenson SK (1991) Applications of hydrologic information automatically extracted from digital elevation models. Hydrol Process 5:31–44. doi:10.1002/hyp.3360050104

Jenson SK, Domingue JO (1988) Extracting topographic structure from digital elevation data for geographic information system analysis. Photogramm Eng Remote Sensing 54(11):1593–1600

León RJ, Bran D, Collantes M, Paruelo JM, Soriano A (1998) Grandes unidades de vegetación de la Patagonia extra andina. Ecologia Austral 8:125–144

Mandelbrot BB (1977) The fractal geometry of nature. W. H. Freeman and Company, New York

Martínez H, Náñez C, Lizuain A, Dal Molin C, Turel A, Dalponte M, Faroux A (2001) Descripción de la Hoja Geológica -San Antonio Oeste, Provincia de Río Negro. SEGEMAR, Buenos Aires

Masoud M (2014) Rainfall-runoff modeling of ungauged Wadis in arid environments (case study Wadi Rabigh-Saudi Arabia). Arab J Geosci 8(5):2587–2606. doi:10.1007/s12517-014-1404-0

Mather PM, Doornkamp JC (1970) Multivariate analysis in geography with particular reference to drainage-basin morphometry. JSTOR 51:163–187. doi:10.2307/621768

Melton MA (1957) An analysis of the relations among elements of climate, surface properties and geomorphology (Tech. Rep. 11). Columbia University, New York

Metz M, Mitasova H, Harmon RS (2011) Efficient extraction of drainage networks from massive, radar-based elevation models with least cost path search. Hydrol Earth Syst Sci 15:667–678. doi:10.5194/hess-15-667-2011

Miller JR, Ritter DF, Kochel RC (1990) Morphometric assessment of lithologic controls on drainage basin evolution in the Crawford upland, South Central Indiana. American J Sci 290:569–599

O'Callaghan J, Mark DM (1984) The extraction of drainage networks from digital elevation data. Comput Vis Graph 28:323–344

Olivares G, Sisul A (2005) Los recursos hídricos en el sector costero rionegrino. In: Freddy Masera R, Lew J, Serra Pirano G (eds) Las

mesetas patagónicas que caen al mar: La costa rionegrina. Gobierno de Río Negro, Río Negro, pp 237–247

Perucca LP, Esper AY (2011) Morphometric characterization of del Molle Basin applied to the evaluation of flash floods hazard, Iglesia Department, San Juan, Argentina. Quat Int 233(1):81–86. doi:10.1016/j.quaint.2010.08.007

Raux J, Copard Y, Laignel B, Fournier M, Masseï N (2011) Classification of worldwide drainage basins through the multivariate analysis of variables controlling their hydrosedimentary response. Global Planet Change 76:117–127. doi:10.1016/j.gloplacha.2010.12.005

Rodriguez-Iturbe I, Rinaldo A (1997) Fractal River Basins: chance and self-organization. Cambridge University Press, Cambridge

Schumm SA (1956) Evolution of drainage systems and slopes in badlands at Perth Amboy, New Jersey. Geol Soc Am Bull 67:597–646

Sener A, Davraz A, Ozcelik M (2005) An integration of GIS and remote sensing in groundwater investigations: a case study in Burdur, Turkey. Hydrogeol J 13:826–834. doi:10.1007/s10040-004-0378-5

Sharma SK, Tignath S, Gajbhiye S, Patil R (2013) Application of principal component analysis in grouping geomorphic parameters of Uttela watershed for hydrological modeling. IJRSG 2(6):63–70

Singh PK, Kumar V, Purohit RC, Kothari M, Dashora PK (2009) Application of principal component analysis in grouping geomorphic parameters for hydrologic modeling. Water Resour Manag 23:325–339. doi:10.1007/s11269-008-9277-1

Sreedevi PD, Sreekanth PD, Khan HH, Ahmed S (2012) Drainage morphometry and its influence on hydrology in an semi arid region: using SRTM data and GIS. Environ Earth Sci 70(2):839–848. doi:10.1007/s12665-012-2172-3

SSRH-INA (2002) Atlas Digital de los Recursos Hídricos Superficiales de la República Argentina. Subsecretaría de Recursos Hídricos de la Nación Instituto Nacional del Agua, Buenos Aires

Strahler AN (1957) Quantitative analysis of watershed geomorphology. Am Geophys Union Trans 38(6):913–920

Strahler AN (1964) Quantitative geomorphology of drainage basins and channel networks. In: Chow VT (ed) Handbook of applied hydrology. McGraw-Hill, New York, pp 439–476

Subyani AM, Qari MH, Matsah MI (2010) Digital elevation model and multivariate statistical analysis of morphometric parameters of some wadis, western Saudi Arabia. Arab J Geosci 5:147–157. doi:10.1007/s12517-010-0149-7

Thomas J, Joseph S, Thrivikramji KP, Abe G (2011) Morphometric analysis of the drainage system and its hydrological implications in the rain shadow regions, Kerala, India. J Geogr Sci 21(6):1077–1088. doi:10.1007/s11442-011-0901-2

Vieceli N, Bortolin TA, Mendes LA, Bacarim G, Cemin G, Schneider VE (2014) Morphometric evaluation of watersheds in Caxias do Sul City, Brazil, using SRTM (DEM) data and GIS. Environ Earth Sci 73(9):5677–5685. doi:10.1007/s12665-014-3823-3

Vogt JV, Colombo R, Bertolo F (2003) Deriving drainage networks and catchment boundaries: a new methodology combining digital elevation data and environmental characteristics. Geomorphology 53(3-4):281–298. doi:10.1016/S0169-555X(02)00319-7

Wheater HS (2007) Modelling hydrological processes in arid and semi-arid areas: an itroduction to the workshop. In: Wheater HS, Sorooshian S, Sharma KD (eds) Hydrological modelling in arid and semi-arid areas, part of international hydrology series. Cambridge University Press, Cambridge, pp 1–19

Wolock DM, Winter TC, Mcmahon G (2004) Delineation and evaluation of hydrologic-landscape regions in the United States using geographic information system tools and multivariate statistical analyses. Environ Manage 34(1):S71–S88. doi:10.1007/s00267-003-5077-9

Yamazaki D, Oki T, Kanae S (2009) Deriving a global river network map and its sub-grid topographic characteristics from a fine-resolution flow direction map. Hydrol Earth Syst Sci 13(11):2241–2251. doi:10.5194/hess-13-2241-2009

Youssef AM, Pradhan B, Hassan AM (2010) Flash flood risk estimation along the St. Katherine road, Southern Sinai, Egypt using GIS based morphometry and satellite imagery. Environ Earth Sci 62(3):611–623. doi:10.1007/s12665-010-0551-1